EUROPEAN ORGANIZATION FOR NUCLEAR RESEARCH

Search for R-parity Violating Chargino and Neutralino Decays in e^+e^- Collisions up to $\sqrt{s} = 183$ GeV

The L3 Collaboration

Abstract

A search for chargino and neutralino pair production in e^+e^- collisions at center-of-mass energies between 161 GeV and 183 GeV is performed under the assumptions that R-parity is not conserved and that only purely leptonic or hadronic R-parity violating decays are allowed. No signal is found in the data. Limits on the production cross sections, on the Minimal Supersymmetric Standard Model parameters and on the masses of the supersymmetric particles are derived.

1 Introduction

The most general superpotential of the Minimal Supersymmetric Standard Model (MSSM) [1], which describes a supersymmetric, renormalizable and gauge invariant theory, with minimal particle content, includes the term W_R [2]:

$$W_R = \lambda_{ijk}L_iL_j\overline{E}_k + \lambda'_{ijk}L_iQ_j\overline{D}_k + \lambda''_{ijk}\overline{U}_i\overline{D}_j\overline{D}_k \,, \tag{1}$$

where λ_{ijk}, λ'_{ijk} and λ''_{ijk} are the Yukawa couplings and i, j and k are the generation indices; L_i and Q_i are the left-handed lepton- and quark-doublet superfields; $\overline{E}_i$, $\overline{D}_i$ and $\overline{U}_i$ are the right-handed singlet superfields for charged leptons, down- and up-type quarks, respectively. In order to prevent the simultaneous presence of identical fermionic fields, the following antisymmetry relations are required: $\lambda_{ijk} = -\lambda_{jik}$ and $\lambda''_{ijk} = -\lambda''_{ikj}$, so that there are in total $9 + 27 + 9$ independent Yukawa couplings.

The λ_{ijk} and λ'_{ijk} couplings violate the leptonic quantum number L, while the λ''_{ijk} couplings violate the baryonic quantum number B. Their simultaneous presence would lead to a fast proton decay [3], which is experimentally excluded [4]. This can be avoided by imposing the conservation of R-parity, a multiplicative quantum number defined as:

$$R = (-1)^{3B+L+2S} \,, \tag{2}$$

where S is the spin. R is $+1$ for all ordinary particles, and -1 for their supersymmetric partners. As a consequence, if R-parity is conserved, supersymmetric particles can be produced only in pairs and they decay in cascade to the lightest supersymmetric particle (LSP), which is stable. However, the absence of either the B-violating or the L-violating terms, or of a subset of them, is enough to prevent a fast proton decay, while allowing the LSP to decay into Standard Model particles via scalar lepton or quark exchange.

In this paper, we search for pair-produced neutralinos ($e^+e^- \to \tilde{\chi}_1^0\tilde{\chi}_1^0$, $e^+e^- \to \tilde{\chi}_i^0\tilde{\chi}_1^0, i \geq 2$) and charginos ($e^+e^- \to \tilde{\chi}_1^+\tilde{\chi}_1^-$) with subsequent R-parity violating decays, assuming that one of the λ_{ijk} or λ''_{ijk} coupling constants is non-negligible. The λ'_{ijk} couplings are not considered. In all processes studied, the lightest neutralino is assumed to decay into three fermions according to the dominant λ_{ijk} or λ''_{ijk} interaction term, as detailed in Table 1. Charginos can decay directly into three fermions, via the dominant R-parity violating term, as listed in Table 1, when the chargino is the LSP or when the R-parity violating coupling is strong enough. If the $\tilde{\chi}_1^0$ is the LSP, charginos can also decay indirectly into $\tilde{\chi}_1^0W^*$, or into $\tilde{\chi}_2^0W^*$ for chargino heavier than the next-to-lightest neutralino. Similarly the heavier neutralinos ($\tilde{\chi}_i^0, i \geq 2$) can decay indirectly into $Z^*\tilde{\chi}_1^0$ or directly into fermions. When the lightest scalar lepton is the LSP, the process $\tilde{\chi}_1^0 \to \ell\tilde{\ell}$ is taken into account for the λ_{ijk} analysis.

Coupling	Neutralino decays	Chargino decays
λ_{ijk}	$\ell_i^-\nu_j\ell_k^+$, $\nu_i\ell_j^+\ell_k^-$	$\nu_i\nu_j\ell_k^+$, $\ell_i^+\ell_j^+\ell_k^-$
λ''_{ijk}	$\bar{u}_i\bar{d}_j\bar{d}_k$	$\bar{d}_i\bar{d}_j\bar{d}_k$, $u_iu_jd_k$, $u_id_ju_k$

Table 1: Allowed R-parity violating direct decays of the neutralino and chargino. Charged conjugate states are implied.

In the present analysis, the dominant coupling is assumed to be greater than 10^{-5} [5], corresponding to decay lengths smaller than 1 cm. Searches for R-parity violating decays have also been performed by other LEP experiments [6].

2 Data and Monte Carlo Samples

The data used corresponds to an integrated luminosity of 55.3 pb^{-1} collected by the L3 detector [7] at the center-of-mass energy ($\sqrt{s}$) of 182.7 GeV, hereafter referred to as 183 GeV. For the indirect λ_{ijk} analysis, 21.1 pb^{-1} of data collected at 161–172 GeV are also used.

The signal events are generated with SUSYGEN [8] for different values of neutralino and chargino masses, for all possible choices of the generation indices.

The following Monte Carlo generators are used to simulate Standard Model processes: PYTHIA [9] for $e^+e^- \to q\bar{q}$, $e^+e^- \to Z e^+e^-$ and $e^+e^- \to ZZ$, BHAGENE3 [10] for $e^+e^- \to e^+e^-$, KORALZ [11] for $e^+e^- \to \mu^+\mu^-$ and $e^+e^- \to \tau^+\tau^-$, PHOJET [12] for $e^+e^- \to e^+e^-q\bar{q}$, DIAG36 [13] for $e^+e^- \to e^+e^-\ell^+\ell^-$ ($\ell = e, \mu, \tau$) and KORALW [14] for $e^+e^- \to W^+W^-$. The number of simulated events corresponds to at least 100 times the luminosity of the data, except for Bhabha and two-photon processes, where the Monte Carlo samples correspond to approximately 5 times the luminosity.

The detector response is simulated using the GEANT package [15]. It takes into account effects of energy loss, multiple scattering and showering in the detector materials. Hadronic interactions are simulated with the GHEISHA program [16]. Time dependent inefficiencies of the different subdetectors are also taken into account in the simulation procedure.

3 Analysis Procedure

3.1 λ_{ijk}: Topology and Preselection

When the λ_{ijk} couplings dominate, the LSP decays into three leptons. The possible topologies arising from the different final states are listed in Table 2. Selections for the different topologies are developed.

Process				Topology
$e^+e^- \to \tilde{\chi}_1^0\tilde{\chi}_1^0 \to$	$\ell\ell\ell\ell\nu\nu$			$4\,\ell + \not{E}$
$e^+e^- \to \tilde{\chi}_i^0\tilde{\chi}_1^0 \to$	$\tilde{\chi}_1^0\tilde{\chi}_1^0\,Z^* \to$	$\ell\ell\ell\ell\nu\nu$	qq	$4\,\ell + 2$ jets $+ \not{E}$
$(i \geq 2)$		$\ell\ell\ell\ell\nu\nu$	$\ell\ell$	$6\,\ell + \not{E}$
		$\ell\ell\ell\ell\nu\nu$	$\nu\nu$	$4\,\ell + \not{E}$
$e^+e^- \to \tilde{\chi}_1^+\tilde{\chi}_1^- \to$	$\tilde{\chi}_1^0\tilde{\chi}_1^0\,W^*W^* \to$	$\ell\ell\ell\ell\nu\nu$	$qq'qq'$	$4\,\ell + 4$ jets $+ \not{E}$
		$\ell\ell\ell\ell\nu\nu$	$qq'\ell\nu$	$5\,\ell + 2$ jets $+ \not{E}$
		$\ell\ell\ell\ell\nu\nu$	$\ell\nu\ell\nu$	$6\,\ell + \not{E}$
$e^+e^- \to \tilde{\chi}_1^+\,\tilde{\chi}_1^- \to$	$\ell\ell\ell\ell\ell\ell$			$6\,\ell$
	$\ell\ell\ell\ell\nu\nu$			$4\,\ell + \not{E}$
	$\ell\ell\nu\nu\nu\nu$			$2\,\ell + \not{E}$

Table 2: Processes and topologies considered in the λ_{ijk} coupling analysis.

The decay products of the $\tilde{\chi}_1^0$ pair are four charged leptons and two neutrinos. If the λ_{133} coupling dominates, each neutralino can decay into $\bar{\nu}_e\tau^+\tau^-$, $\nu_\tau e^+\tau^-$, $\nu_e\tau^-\tau^+$ or $\bar{\nu}_\tau e^-\tau^+$, and the final state contains at least two τ leptons, which are selected with lower efficiency with respect to electrons and muons. If the neutralino mass is high ($M_{\tilde{\chi}_1^0} \geq 50$ GeV) the event topology consists of four charged leptons, isotropically distributed, and missing energy ($\not{E}$). On the contrary, for low neutralino masses ($M_{\tilde{\chi}_1^0} \leq 20$ GeV) the events consist of two back-to-

back lepton pairs and missing energy. In this case, there is a large background from Standard Model lepton-pair processes.

In the case of the process $e^+e^- \to \tilde{\chi}_i^0 \tilde{\chi}_1^0 \to \tilde{\chi}_1^0 Z^* \tilde{\chi}_1^0$, three possible final states are present, corresponding to the Z^* decays into hadrons, charged leptons or neutrinos. As is shown in Table 2, the topologies arising from this process include leptons and missing energy or leptons plus hadronic jets and missing energy. These topologies are covered by combining the neutralino and chargino pair selections, described below.

In the case of chargino production, the signal topologies depend not only on the values of the chargino and neutralino masses, but also on the chargino decay modes. For small values of the mass difference $\Delta M = M_{\tilde{\chi}_1^\pm} - M_{\tilde{\chi}_1^0}$ ($\Delta M \leq 10$ GeV) the event energy is mainly carried by the neutralino decay products, almost independently of the different chargino decay channels. Therefore, a common selection is developed for all chargino decay modes. On the contrary, for medium and large ΔM values ($\Delta M > 10$ GeV), different selections are developed for each possible configuration. As the process $e^+e^- \to q\bar{q}$ and hadronic W^+W^- decays are the main background for the hadronic mode, a relatively low multiplicity is required.

In the case of chargino R-parity violating direct decays, three possible topologies can occur. When both charginos decay into three charged leptons, the final state is almost background free. If the decay products are two charged leptons and four neutrinos, the main background contributions come from leptonic W and τ decays and two-photon interactions. The last topology, four charged leptons plus missing energy, is already taken into account by the neutralino pair selection.

Events are preselected by requiring at least 3 charged tracks and 4 calorimetric clusters in order to remove $e^+e^- \to e^+e^-, \mu^+\mu^-$ and purely leptonic $\tau^+\tau^-$ and W^+W^- decays. Events have to contain at least two charged leptons. The visible energy has to be smaller than 90% of $\sqrt{s}$ in order to remove high multiplicity $q\bar{q}$ events and hadronic W^+W^- and ZZ decays. The missing momentum vector is required to be in the polar angle range between $5°$ and $175°$. In order to reject cosmic ray interactions, at least one time of flight measurement is required to be consistent with the beam crossing.

Special care is taken in order to reduce the background contribution from two-photon interactions. Tagged two-photon interactions are rejected by requiring the sum of the energies measured in the small angle calorimeters between $1.5°$ and $9.0°$ to be less than 10 GeV. In addition, the visible energy must be greater than 15% of $\sqrt{s}$. Background from two-photon collisions is further reduced by requiring the transverse missing momentum to be greater than 5 GeV.

After the preselection is applied, 337 events are selected in the data sample and 334 events are expected in total from Standard Model processes. The signal preselection efficiency for $e^+e^- \to \tilde{\chi}_1^+ \tilde{\chi}_1^-$ is about 85% for $M_{\tilde{\chi}_1^\pm} = 91$ GeV, at $\sqrt{s} = 183$ GeV. For $e^+e^- \to \tilde{\chi}_1^0 \tilde{\chi}_1^0$ the efficiency is greater than 80% for $M_{\tilde{\chi}_1^0} \geq 50$ GeV and between 35% and 60% for 5 GeV$\leq M_{\tilde{\chi}_1^0} \leq$ 20 GeV. Figure 1 shows the number of tracks, number of leptons, normalised visible energy and $\ln(y_{34})$ distributions after the preselection. The jet resolution parameter y_{mn} is defined as the y_{cut} value at which the event configuration changes from n to m jets, when using the DURHAM [17] clustering scheme. The data are in good agreement with the Monte Carlo expectations.

3.2 λ''_{ijk}: Topology and Preselection

If λ''_{ijk} couplings dominate, the LSP decays into three quarks, with a flavour composition given by the generation indices of the dominant λ''_{ijk} coupling. The possible topologies arising from the different final states are summarized in Table 3.

Process	Topology
$e^+e^- \rightarrow \tilde{\chi}^0_1\tilde{\chi}^0_1$ or $\tilde{\chi}^+_1\tilde{\chi}^-_1 \rightarrow qqqqqq$	2 jets
	4 jets
	6 jets
$e^+e^- \rightarrow \tilde{\chi}^0_i\tilde{\chi}^0_1 \rightarrow \tilde{\chi}^0_1\tilde{\chi}^0_1 \, Z^* \rightarrow qqqqqq \, ff$ $(i \geq 2)$	4 jets or 6 jets
	(4 or 6) jets + leptons
	(4 or 6) jets + $\not{E}$
$e^+e^- \rightarrow \tilde{\chi}^+_1\tilde{\chi}^-_1 \rightarrow \tilde{\chi}^0_1\tilde{\chi}^0_1 \, W^*W^* \rightarrow qqqqqq \, ff'f''f'''$	4 jets or 6 jets
	(4 or 6) jets + lepton(s) + $\not{E}$

Table 3: Processes and topologies considered in the λ''_{ijk} coupling analyses for events containing two, four or six resolved jets.

In the case of $\tilde{\chi}^0_1$ pair production, the final state contains six quarks, and three different topologies can occur, depending on the value of $M_{\tilde{\chi}^0_1}$. For low and medium neutralino masses ($M_{\tilde{\chi}^0_1} \leq 50$ GeV) not all the six jets in the event can be resolved, while for high masses ($M_{\tilde{\chi}^0_1} > 50$ GeV) they can be well separated. Therefore, the signal topology is two-jet like for small values of the neutralino mass. For intermediate neutralino masses the events are more similar to four jets, while for large neutralino masses the events can contain six isolated jets, isotropically distributed. For small neutralino masses the main background contribution comes from $e^+e^- \rightarrow q\bar{q}$. When the signal topology is four-jet like, $q\bar{q}gg$ and hadronic W^+W^- decays contribute. For high neutralino masses, the most important background source is W^+W^- events.

The same multi-jet topology occurs when charginos decay directly into three quarks, or when the mass difference ΔM is sufficiently small, so that the decay products of the W^* pair carry only a negligible fraction of the event energy. Since charginos of masses up to 45 GeV are excluded by Z lineshape measurements [18], the two-jet topology is not addressed in this case. Analogous considerations apply for the processes $\tilde{\chi}^0_2\tilde{\chi}^0_1$ and $\tilde{\chi}^0_3\tilde{\chi}^0_1$. When ΔM is large, leptons and neutrinos from W^* decays can carry a relevant fraction of the event energy, leading to lower selection efficiencies.

In this analysis no attempt is made to identify quark flavours. However, the efficiency is found to be slightly higher for events containing b-quarks than for events with light quarks. Therefore, only the results obtained by the choice $\lambda''_{ijk} = \lambda''_{112}$ will be quoted in the next sections.

The preselection of the λ''_{ijk} analysis aims at selecting well balanced hadronic events. Low multiplicity events, like leptonic Z and W decays, are rejected by requiring at least 13 calorimetric clusters. At least one charged track has to be present. The visible energy has to be greater than 50% of $\sqrt{s}$. The energy imbalances, parallel and perpendicular to the beam direction, are required to be smaller than 20% of the visible energy.

Above the Z peak a large fraction of background events contains a hard initial state radiation (ISR) photon. Unbalanced events with an ISR photon in the beam pipe are removed by means of the requirement on the parallel energy imbalance. In order to reject events with an ISR photon seen in the detector, the invariant mass of the hadronic system has to be greater than

80% of $\sqrt{s}$.

In order to remove background contributions from two-photon interactions, the energy in a cone of 12° half opening angle around the beam axis must not exceed 30% of the total visible energy. Furthermore, the thrust axis is required to be well contained in the detector with a polar angle between 8° and 172°.

After the preselection is applied, 1953 events are selected in the data sample and 1949 are expected from Standard Model processes, mainly coming from $q\bar{q}$ and W^+W^- events. The signal preselection efficiency for $e^+e^- \rightarrow \tilde{\chi}_1^0 \tilde{\chi}_1^0$ is about 85% and for $e^+e^- \rightarrow \tilde{\chi}_1^+ \tilde{\chi}_1^-$ is between 60% and 90%, at $\sqrt{s} = 183$ GeV. Figure 2 shows the $\ln(y_{34})$, thrust, $\ln(y_{45})$ and narrow jet broadening (B_N) [19] distributions after the preselection. There is a good agreement between data and Monte Carlo expectations.

3.3 Analysis Optimization

After the preselection level, dedicated selections are performed to maximize the λ_{ijk} and λ''_{ijk} analysis sensitivities according to the topologies arising from those couplings.

In the λ_{ijk} case, thirteen selections are performed for which the cut values of the following variables are optimized simultaneously: acollinearity and acoplanarity angles, thrust, y_{34} and polar angle of the missing momentum. The acollinearity and acoplanarity angles are calculated by reconstructing every event into exactly two jets with the DURHAM algorithm.

Fourteen selections are performed for the λ''_{ijk} analysis. The sum of the di-jet masses is required not to be consistent with W^+W^- pair production. For the λ''_{ijk} neutralino selection, the optimization procedure includes the following variables: thrust, wide jet broadening variable, y_{34} and y_{45}. For the λ''_{ijk} chargino selection, the cut values of the following variables are optimized: thrust, B_N, y_{34} and y_{56}.

The optimization procedure uses Monte Carlo signal and background events and is described in Reference 20. For two-photon interactions, which represent an important background source for the λ_{ijk} analysis, the optimization and the background estimation are performed on two independent samples to avoid potential biases from statistical fluctuations.

3.4 Efficiencies

Here we discuss only the results obtained for $\lambda_{ijk} = \lambda_{133}$ and $\lambda''_{ijk} = \lambda''_{112}$, since these choices of the generation indices give the lowest selection efficiencies. In the following, only the efficiencies at $\sqrt{s} = 183$ GeV are quoted for simplicity. The efficiencies of the processes $e^+e^- \rightarrow \tilde{\chi}_1^0 \tilde{\chi}_1^0$, $e^+e^- \rightarrow \tilde{\chi}_1^+ \tilde{\chi}_1^-$ and $e^+e^- \rightarrow \tilde{\chi}_i^0 \tilde{\chi}_1^0$ are summarized in Tables 4 and 5 for direct and indirect R-parity violating decays.

In the case of direct R-parity violating decays, the efficiencies are estimated for different lightest neutralino or chargino masses. For both λ_{133} and λ''_{112} mediated decays, the efficiencies increase with increasing lightest neutralino or chargino mass. At high masses, six fermions are expected to be isotropically produced and can be disentangled from W-pair production background events. For low masses, the signal signatures look like back-to-back jet events and the selection efficiencies are smaller due to the dominant background coming from the two-fermion processes. In addition, for the λ_{133} selection the efficiencies obtained for low masses (below 50 GeV) are higher for chargino than for neutralino due to the contribution of the six charged lepton final state.

In the case of indirect R-parity violating decays for both charginos and next-to-lightest neutralinos, the efficiencies are estimated for different masses and ΔM ranges. For a chargino mass of 91 GeV and assuming $\tilde{\chi}_1^\pm \to \tilde{\chi}_1^0 W^*$ or $\tilde{\chi}_1^\pm \to \tilde{\chi}_2^0 W^* \to \tilde{\chi}_1^0 Z^* W^*$, the efficiencies obtained for λ_{133} and λ''_{112} mediated decays decrease with increasing ΔM. At high ΔM, the signal signatures are very similar to those of W-pair production. For $M_{\tilde{\chi}_i^0} + M_{\tilde{\chi}_1^0} = 180$ GeV, the efficiencies of the process $e^+e^- \to \tilde{\chi}_i^0 \tilde{\chi}_1^0$ $(i = 2, 3, 4)$ decrease slightly with increasing ΔM for the λ_{133} and λ''_{112} analyses. In the latter case, the efficiencies are smaller compared to those obtained for charginos due to the invisible or purely leptonic Z^* decays.

Coupling	Process	$M_{\tilde{\chi}} = 5$–25 GeV	$M_{\tilde{\chi}} = 25$–55 GeV	$M_{\tilde{\chi}}=55$–91 GeV
λ_{133}	$\tilde{\chi}_1^0 \tilde{\chi}_1^0$	3%–10%	10%–33%	39%–55%
λ_{133}	$\tilde{\chi}_1^+ \tilde{\chi}_1^-$	10%–18%	21%–40%	43%–54%
λ''_{112}	$\tilde{\chi}_1^0 \tilde{\chi}_1^0,\ \tilde{\chi}_1^+ \tilde{\chi}_1^-$	19%–22%	23%–24%	21%–32%

Table 4: Efficiency ranges of $\tilde{\chi}_1^0 \tilde{\chi}_1^0$ and $\tilde{\chi}_1^+ \tilde{\chi}_1^-$ selections for direct R-parity violating neutralino and chargino decays, at $\sqrt{s} = 183$ GeV. In case of the process $\tilde{\chi}_1^+ \tilde{\chi}_1^-$, the lowest mass value considered is $M_{\tilde{\chi}_1^\pm} = 15$ GeV for λ_{133} and 45 GeV for λ''_{112}.

Coupling	Process	$\Delta M = 5$–20 GeV	$\Delta M = 20$–50 GeV	$\Delta M = 50$–80 GeV
λ_{133}	$\tilde{\chi}_i^0 \tilde{\chi}_1^0$	47%–54%	42%–47%	26%–37%
λ_{133}	$\tilde{\chi}_1^+ \tilde{\chi}_1^-$	47%–56%	28%–47%	17%–26%
λ''_{112}	$\tilde{\chi}_i^0 \tilde{\chi}_1^0$	31%–32%	28%–30%	28%–24%
λ''_{112}	$\tilde{\chi}_1^+ \tilde{\chi}_1^-$	30%–43%	45%–51%	10%–43%

Table 5: Efficiency ranges of $\tilde{\chi}_i^0 \tilde{\chi}_1^0$ and $\tilde{\chi}_1^+ \tilde{\chi}_1^-$ selections for indirect R-parity violating neutralino and chargino decays, at $\sqrt{s} = 183$ GeV. The chargino selection efficiencies correspond to $M_{\tilde{\chi}_1^\pm} = 91$ GeV. For the process $\tilde{\chi}_i^0 \tilde{\chi}_1^0$ the efficiencies correspond to $M_{\tilde{\chi}_i^0} + M_{\tilde{\chi}_1^0} = 180$ GeV.

Coupling	Process	$N_{background}$	N_{data}
λ_{ijk}	$\tilde{\chi}_1^0 \tilde{\chi}_1^0$	1.3 ± 0.1	0
λ_{ijk}	$\tilde{\chi}_1^+ \tilde{\chi}_1^-$ (indirect)	1.6 ± 0.1	0
λ_{ijk}	$\tilde{\chi}_1^+ \tilde{\chi}_1^-$ (direct)	10.4 ± 0.5	10
λ''_{ijk}	$\tilde{\chi}_1^0 \tilde{\chi}_1^0$	62 ± 2	52
λ''_{ijk}	$\tilde{\chi}_1^+ \tilde{\chi}_1^-$	46 ± 1	40

Table 6: Number of expected background and observed data events for the different selections.

4 Results

The summary of the searches is given in Table 6, showing the number of candidates and expected background events. We do not observe any excess of events. Therefore we set upper limits on the neutralino and chargino production cross sections assuming direct or indirect R-parity violating decays. We also derive limits on the masses of these particles in the framework of the MSSM. Exclusion limits at 95% C.L. are derived taking into account all the background sources, but the two-photon processes due to the large statistical error. Systematic errors on the signal efficiency are evaluated as in Reference 20. The typical relative error is 5% and is dominated by Monte Carlo statistics. It is taken into account in the calculations of the signal upper limits [21].

4.1 Upper Limits on Neutralino and Chargino Production Cross Sections

The 95% C.L. upper limits on neutralino and chargino pair-production cross sections, both for λ_{ijk} and λ''_{ijk}, are shown in Figure 3. For the λ_{ijk} analysis, the lower center of mass energies are included in the exclusion assuming a constant production cross section.

In the case of dominant λ_{ijk} coupling, the neutralino pair-production cross section is below 0.2 pb at 95% C.L. for $M_{\tilde{\chi}^0_1} \geq 40$ GeV and below 0.1 pb for $M_{\tilde{\chi}^0_1} \geq 60$ GeV. The chargino cross section is below 0.4 pb for a chargino mass greater than 45 GeV in the direct decay mode and is below 0.2 pb for $M_{\tilde{\chi}^\pm_1} = 91$ GeV and $\Delta M \leq 50$ GeV in the indirect decay mode.

In the case of dominant λ''_{ijk} coupling, the neutralino cross section is below 0.6 pb at 95% C.L. for any value of the neutralino mass. The chargino cross section is below 0.6 pb for a chargino mass greater than 45 GeV in the direct decay mode and is below 0.4 pb for $M_{\tilde{\chi}^\pm_1} = 91$ GeV and $\Delta M \leq 60$ GeV in the indirect decay mode.

4.2 Interpretation in the MSSM

The results are also interpreted as excluded regions in the MSSM parameter space. In the MSSM framework neutralino and chargino masses, couplings and cross sections depend on the gaugino mass parameter, M_2, the higgsino mass mixing parameter, μ, the ratio of the vacuum expectation values of the two Higgs doublets, $\tan\beta$, and the common mass of the scalar fermions at the GUT scale, m_0. Therefore the exclusion regions can be expressed in the $M_2 - \mu$ plane for a given value of m_0 and $\tan\beta$. The results presented here hold for λ_{ijk} and $\lambda''_{ijk} > 10^{-5}$ and for $0 \leq M_2 \leq 2000$ GeV, -500 GeV $\leq \mu \leq 500$ GeV. They do not depend on the value of the trilinear coupling in the Higgs sector, A.

In addition to the limits obtained with this analysis, we take into account the constraints from L3 cross section measurements at the Z pole. A point in the MSSM parameter space is excluded at 95% C.L. by Z lineshape measurements if:

$$\left(\frac{\sigma_{SUSY}}{\sigma_{SM}}\right) \Gamma_Z > \Gamma_{LIM} , \tag{3}$$

where σ_{SUSY} is the sum of the pair-production cross sections of supersymmetric particles at $\sqrt{s} = 91$ GeV, calculated with `SUSYGEN` [8], and σ_{SM} is the total Z cross section predicted by the Standard Model. Γ_Z and $\Gamma_{LIM} = 24$ MeV are the measured total Z width and the 95% C.L. upper limit on possible non-Standard Model contributions to the total Z width [18]. Figure 4

shows the exclusion regions at 95% C.L. in the $M_2 - \mu$ plane for $\tan\beta = \sqrt{2}$ and for $m_0 = 60$ GeV or 500 GeV, for both λ_{ijk} and λ''_{ijk}. The excluded regions with the present results are dominated by the chargino analyses. Moreover some regions beyond the chargino kinematic limit are excluded at large m_0 and low $\tan\beta$ values by the $\tilde{\chi}^0_2\tilde{\chi}^0_1$ and $\tilde{\chi}^0_3\tilde{\chi}^0_1$ analyses and at low m_0 by the $\tilde{\chi}^0_1\tilde{\chi}^0_1$ analyses.

Lower limits on the masses of the supersymmetric particles are reported for the following two regions of the parameter space where:

1) the $\tilde{\chi}^0_1$ is the LSP (50 GeV$\leq m_0 \leq$ 500 GeV and any $\tan\beta$
                  or   any m_0 and $2 \leq \tan\beta \leq 40$);

2) the lightest scalar lepton can be the LSP ($0 \leq m_0 < 50$ GeV and $1 \leq \tan\beta < 2$).

In region 2), in the presence of dominant λ_{ijk} coupling the decay chain $\tilde{\chi}^0_1 \to \ell\tilde{\ell} \to \ell\ell\nu$ leads to the same final states arising from neutralino direct R-parity violating decays, so that the analysis is efficient also when the lightest scalar lepton is the LSP. The additional contribution of the process $\tilde{\chi}^0_3\tilde{\chi}^0_1 \to \ell\tilde{\ell}\tilde{\chi}^0_1$ is taken into account for the region in which $M_{\tilde{\ell}} < M_{\tilde{\chi}^0_3}$. When the λ''_{ijk} coupling dominate, the decay $\tilde{\chi}^0_1 \to \ell\tilde{\ell} \to \ell\ell$qqq occurs. Since there is no event generator available for this process, we quote two sets of mass limits for λ''_{ijk} coupling, for region 1) and region 2), respectively.

Figure 5 shows the 95% C.L. lower limits on neutralino and chargino masses as a function of $\tan\beta$. In region 1), we derive the following lower limits at 95% C.L. on the neutralino and chargino masses:

$M_{\tilde{\chi}^0_1} > 26.8$ GeV,
$M_{\tilde{\chi}^0_2} > 44.3$ GeV,
$M_{\tilde{\chi}^\pm_1} > 91.1$ GeV (λ_{ijk} analysis), $M_{\tilde{\chi}^\pm_1} > 90.9$ GeV (λ''_{ijk} analysis).

In region 2), the 95% C.L. lower limits on the neutralino and chargino masses set by the λ''_{ijk} analysis are:

$M_{\tilde{\chi}^0_1} > 26.8$ GeV,
$M_{\tilde{\chi}^0_2} > 34.8$ GeV,
$M_{\tilde{\chi}^\pm_1} > 76.9$ GeV.

From the exclusion contours in the $M_2 - m_0$ plane we set an indirect lower limit on the mass of the lightest scalar lepton. Figure 6 shows the 95% C.L. lower limits on the mass of the supersymmetric partner of the right-handed electron ($M_{\tilde{e}_R}$) for $\tan\beta = 2$. These limits hold also for $\tan\beta > 2$. Figure 7 shows the 95% C.L. lower limit on the scalar electron mass as a function of $\tan\beta$. In region 1), we obtain the following lower limits:

$M_{\tilde{e}_R} > 79.3$ GeV (λ_{ijk} analysis) and $M_{\tilde{e}_R} > 73.0$ GeV (λ''_{ijk} analysis),

while in region 2) the 95% C.L. limits are:

$M_{\tilde{e}_R} > 61.8$ GeV (λ_{ijk} analysis) and $M_{\tilde{e}_R} > 29.5$ GeV (λ''_{ijk} analysis).

The search for neutralino and chargino R-parity violating decays reaches at least the same sensitivity as in the R-parity conserving case [22]. Therefore, the supersymmetry limits obtained at LEP are independent of R-parity conservation assumptions.

Acknowledgements

We wish to express our gratitude to the CERN accelerator division for the excellent performance of the LEP machine. We acknowledge the effort of the engineers and technicians who have participated in the construction and maintenance of this experiment.

References

[1] A review can be found for example in:
H.E. Haber and G.L. Kane, Phys. Rep. **117** (1985) 75.

[2] C.S. Aulakh and R.N. Mohapatra, Phys. Lett. **B 119** (1982) 316;
F. Zwirner, Phys. Lett. **B 132** (1983) 103;
L.J. Hall and M. Suzuki, Nucl. Phys. **B 231** (1984) 419;
R. Barbieri and A. Masiero, Nucl. Phys. **B 267** (1986) 679.
For a recent review and a reference to the literature:
H. Dreiner, "An introduction to explicit R-parity violation", hep–ph/9707435, published in *Perspectives on Supersymmetry*, ed. G.L. Kane, World Scientific, Singapore.

[3] S. Weinberg, Phys. Rev. **D 26** (1982) 287;
G. Bhattacharyya and P.B. Pal, "Upper bounds on all R-parity violating $\lambda\lambda''$ combinations from proton stability", hep–ph/9809493.

[4] Particle Data Group, C. Caso *et al.*, Eur. Phys. J. **C 3** (1998) 1.

[5] S. Dawson, Nucl. Phys. **B 261** (1985) 297.

[6] ALEPH Collab., D. Buskulic *et al.*, Phys. Lett. **B 349** (1995) 238;
ALEPH Collab., R. Barate *et al.*, Eur. Phys. J. **C 4** (1998) 433;
ALEPH Collab., R. Barate *et al.*, CERN-EP/98-147, subm. to Eur. Phys. J. **C**;
OPAL Collab., G. Abbiendi *et al.*, CERN-EP/98-203 subm. to Eur. Phys. J. **C**.

[7] L3 Collab., B. Adeva *et al.*, Nucl. Instr. and Meth. **A 289** (1990) 35;
J.A. Bakker *et al.*, Nucl. Instr. and Meth. **A 275** (1989) 81;
O. Adriani *et al.*, Nucl. Instr. and Meth. **A 302** (1991) 53;
B.Adeva *et al.*, Nucl. Instr. and Meth. **A 323** (1992) 109;
K. Deiters *et al.*, Nucl. Instr. and Meth. **A 323** (1992) 162;
M. Chemarin *et al.*, Nucl. Instr. and Meth. **A 349** (1994) 345;
M. Acciarri *et al.*, Nucl. Instr. and Meth. **A 351** (1994) 300;
G. Basti *et al.*, Nucl. Instr. and Meth. **A 374** (1996) 293;
I.C. Brock *et al.*, Nucl. Instr. and Meth. **A 381** (1996) 236;
A. Adam *et al.*, Nucl. Instr. and Meth. **A 383** (1996) 342.

[8] S. Katsanevas and S. Melachroinos, Proceedings of the Workshop "Physics at LEP 2", eds. G. Altarelli, T. Sjöstrand and F. Zwirner, CERN 96-01 (1996), vol. 2, p. 328.
`SUSYGEN 2.2`, S. Katsanevas and P. Morawitz, Comp. Phys. Comm. **112** (1998) 227.

[9] `PYTHIA 5.7` and `JETSET 7.4` Physics and Manual, T. Sjöstrand, CERN-TH/7112/93 (1993), revised August 1995; Comp. Phys. Comm. **82** (1994) 74.

[10] BHAGENE3: Version 3 was used. J.H. Field, Phys. Lett. **B 323** (1994) 432;
J.H. Field and T. Riemann, Comp. Phys. Comm. **94** (1996) 53.

[11] KORALZ: Version 4.02 was used. S. Jardach, B.F.L. Ward, and Z. Wąs, Comp. Phys. Comm. **79** (1994) 503.

[12] PHOJET: Version 1.05 was used. R. Engel, Z. Phys. **C 66** (1995) 203;
R. Engel and J. Ranft, Phys. Rev. **D 54** (1996) 4244.

[13] DIAG36: F.A. Berends, P.H. Daverfeldt and R. Kleiss, Nucl. Phys. **B 253** (1985) 441.

[14] KORALW: Version 1.21 was used. M. Skrzypek, S. Jardach, W. Placzek, and Z. Wąs, Comp. Phys. Comm. **94** (1996) 216;
M. Skrzypek, S. Jardach, M. Martinez, W. Placzek, and Z. Wąs, Phys. Lett. **B 372** (1996) 289.

[15] GEANT: Version 3.15 was used. R. Brun et al, CERN DD/EE/84-1 (Revised 1987).

[16] H. Fesefeldt, RWTH Aachen Report PITHA 85/2 (1985).

[17] Yu. L. Dokshitzer, Contribution to the Workshop on Jets at LEP and HERA (1990);
N. Brown and W.J. Stirling, Rutherford Preprint RAL-91-049;
S. Catani *et al.*, Phys. Lett. **B 269** (1991) 432;
S. Bethke *et al.*, Nucl. Phys. **B 370** (1992) 310.

[18] L3 Collab., M. Acciarri *et al.*, Z. Phys. **C 62** (1994) 223.

[19] L3 Collab., M.Acciari *et al.*, Phys. Lett. **B 444** (1998) 569.

[20] L3 Collab., M. Acciarri *et al.*, Phys. Lett. **B 377** (1996) 289.

[21] R.D. Cousins and V.L. Highland, Nucl. Instr. and. Meth. **A 320** (1992) 331.

[22] L3 Collab., M. Acciarri *et al.*, Search for Charginos and Neutralinos in e^+e^- Collisions at $\sqrt{s} = 161$–183 GeV, paper in preparation:
L3 Collab., contributed paper number 493 to ICHEP98, UBC, Vancouver, B.C., Canada, July 1998.

The L3 Collaboration:

M.Acciarri[26] P.Achard[18] O.Adriani[15] M.Aguilar-Benitez[25] J.Alcaraz[25] G.Alemanni[21] J.Allaby[16] A.Aloisio[28] M.G.Alviggi[28] G.Ambrosi[18] H.Anderhub[47] V.P.Andreev[6,36] T.Angelescu[12] F.Anselmo[9] A.Arefiev[27] T.Azemoon[3] T.Aziz[10] P.Bagnaia[35] L.Baksay[42] A.Balandras[4] R.C.Ball[3] S.Banerjee[10] Sw.Banerjee[10] K.Banicz[44] A.Barczyk[47,45] R.Barillère[16] L.Barone[35] P.Bartalini[21] M.Basile[9] R.Battiston[32] A.Bay[21] F.Becattini[15] U.Becker[14] F.Behner[47] J.Berdugo[25] P.Berges[14] B.Bertucci[32] B.L.Betev[47] S.Bhattacharya[10] M.Biasini[32] A.Biland[47] J.J.Blaising[4] S.C.Blyth[33] G.J.Bobbink[2] A.Böhm[1] L.Boldizsar[13] B.Borgia[16,35] D.Bourilkov[47] M.Bourquin[18] S.Braccini[18] J.G.Branson[38] V.Brigljevic[47] F.Brochu[4] A.Buffini[15] A.Buijs[43] J.D.Burger[14] W.J.Burger[32] J.Busenitz[42] A.Button[3] X.D.Cai[14] M.Campanelli[47] M.Capell[14] G.Cara Romeo[9] G.Carlino[28] A.M.Cartacci[15] J.Casaus[25] G.Castellini[15] F.Cavallari[35] N.Cavallo[28] C.Cecchi[18] M.Cerrada[25] F.Cesaroni[22] M.Chamizo[18] Y.H.Chang[49] U.K.Chaturvedi[17] M.Chemarin[24] A.Chen[49] G.Chen[7] G.M.Chen[7] H.F.Chen[19] H.S.Chen[7] X.Chereau[4] G.Chiefari[28] L.Cifarelli[37] F.Cindolo[9] C.Civinini[15] I.Clare[14] R.Clare[14] G.Coignet[4] A.P.Colijn[2] N.Colino[25] S.Costantini[8] F.Cotorobai[12] B.Cozzoni[9] B.de la Cruz[25] A.Csilling[13] T.S.Dai[14] J.A.van Dalen[30] R.D'Alessandro[15] R.de Asmundis[28] P.Deglon[18] A.Degré[4] K.Deiters[45] D.della Volpe[28] P.Denes[34] F.DeNotaristefani[35] A.De Salvo[47] M.Diemoz[35] D.van Dierendonck[2] F.Di Lodovico[47] C.Dionisi[16,35] M.Dittmar[47] A.Dominguez[38] A.Doria[28] M.T.Dova[17,♯] D.Duchesneau[4] D.Dufournand[4] P.Duinker[2] I.Duran[39] H.El Mamouni[24] A.Engler[33] F.J.Eppling[14] F.C.Erné[2] P.Extermann[18] M.Fabre[45] R.Faccini[35] M.A.Falagan[25] S.Falciano[35] A.Favara[15] J.Fay[24] O.Fedin[36] M.Felcini[47] T.Ferguson[33] F.Ferroni[35] H.Fesefeldt[1] E.Fiandrini[32] J.H.Field[18] F.Filthaut[16] P.H.Fisher[14] I.Fisk[38] G.Forconi[14] L.Fredj[18] K.Freudenreich[47] C.Furetta[26] Yu.Galaktionov[27,14] S.N.Ganguli[10] P.Garcia-Abia[5] M.Gataullin[31] S.S.Gau[11] S.Gentile[35] N.Gheordanescu[12] S.Giagu[35] Z.F.Gong[19] G.Grenier[24] M.W.Gruenewald[8] R.van Gulik[2] V.K.Gupta[34] A.Gurtu[10] L.J.Gutay[44] D.Haas[5] A.Hasan[29] D.Hatzifotiadou[9] T.Hebbeker[8] A.Hervé[16] P.Hidas[13] J.Hirschfelder[33] H.Hofer[47] G. Holzner[47] H.Hoorani[33] S.R.Hou[49] I.Iashvili[46] B.N.Jin[7] L.W.Jones[3] P.de Jong[2] I.Josa-Mutuberría[25] R.A.Khan[17] D.Kamrad[46] J.S.Kapustinsky[23] M.Kaur[17,◇] M.N.Kienzle-Focacci[18] D.Kim[35] D.H.Kim[41] J.K.Kim[41] S.C.Kim[41] W.W.Kinnison[23] J.Kirkby[16] D.Kiss[13] W.Kittel[30] A.Klimentov[14,27] A.C.König[30] A.Kopp[46] I.Korolko[27] V.Koutsenko[14,27] R.W.Kraemer[33] W.Krenz[1] A.Kunin[14,27] P.Lacentre[46,♮,♯] P.Ladron de Guevara[25] I.Laktineh[24] G.Landi[15] K.Lassila-Perini[47] P.Laurikainen[20] A.Lavorato[37] M.Lebeau[16] A.Lebedev[14] P.Lebrun[24] P.Lecomte[47] P.Lecoq[16] P.Le Coultre[47] H.J.Lee[8] J.M.Le Goff[16] R.Leiste[46] E.Leonardi[35] P.Levtchenko[36] C.Li[19] C.H.Lin[49] W.T.Lin[49] F.L.Linde[2,16] L.Lista[28] Z.A.Liu[7] W.Lohmann[46] E.Longo[35] Y.S.Lu[7] K.Lübelsmeyer[1] C.Luci[16,35] D.Luckey[14] L.Lugnier[24] L.Luminari[35] W.Lustermann[47] W.G.Ma[19] M.Maity[10] G.Majumder[10] L.Malgeri[16] A.Malinin[27] C.Maña[25] D.Mangeol[30] P.Marchesini[47] G.Marian[42,¶] J.P.Martin[24] F.Marzano[35] G.G.G.Massaro[2] K.Mazumdar[10] R.R.McNeil[6] S.Mele[16] L.Merola[28] M.Meschini[15] W.J.Metzger[30] M.von der Mey[1] D.Migani[9] A.Mihul[12] H.Milcent[16] G.Mirabelli[35] J.Mnich[16] P.Molnar[8] B.Monteleoni[15] T.Moulik[10] G.S.Muanza[24] F.Muheim[18] A.J.M.Muijs[2] M.Napolitano[28] F.Nessi-Tedaldi[47] H.Newman[31] T.Niessen[1] A.Nisati[35] H.Nowak[46] Y.D.Oh[41] G.Organtini[35] R.Ostonen[20] C.Palomares[25] D.Pandoulas[1] S.Paoletti[35,16] P.Paolucci[28] H.K.Park[33] I.H.Park[41] G.Pascale[35] G.Passaleva[16] S.Patricelli[28] T.Paul[11] M.Pauluzzi[32] C.Paus[16] F.Pauss[47] D.Peach[16] M.Pedace[35] Y.J.Pei[35] S.Pensotti[26] D.Perret-Gallix[4] B.Petersen[30] S.Petrak[8] D.Piccolo[28] M.Pieri[15] P.A.Piroué[34] E.Pistolesi[26] V.Plyaskin[27] M.Pohl[47] V.Pojidaev[27,15] H.Postema[14] J.Pothier[16] N.Produit[18] D.Prokofiev[36] J.Quartieri[37] G.Rahal-Callot[47] N.Raja[10] P.G.Rancoita[26] G.Raven[38] P.Razis[29]D.Ren[47] M.Rescigno[35] S.Reucroft[11] T.van Rhee[43] S.Riemann[46] K.Riles[3] A.Robohm[47] J.Rodin[42] B.P.Roe[3] L.Romero[25] S.Rosier-Lees[4] J.A.Rubio[16] D.Ruschmeier[8] H.Rykaczewski[47] S.Sakar[35] J.Salicio[16] E.Sanchez[16] M.P.Sanders[30] M.E.Sarakinos[20] C.Schäfer[1] V.Schegelsky[36] S.Schmidt-Kaerst[1] D.Schmitz[1] N.Scholz[47] H.Schopper[48] D.J.Schotanus[30] J.Schwenke[1] G.Schwering[1] C.Sciacca[28] D.Sciarrino[18] A.Seganti[9] L.Servoli[32] S.Shevchenko[31] N.Shivarov[40] V.Shoutko[27] J.Shukla[23] E.Shumilov[27] A.Shvorob[31] T.Siedenburg[1] D.Son[41] B.Smith[33] P.Spillantini[15] M.Steuer[14] D.P.Stickland[34] A.Stone[6] H.Stone[34] B.Stoyanov[40] A.Straessner[1] K.Sudhakar[10] G.Sultanov[17] L.Z.Sun[19] H.Suter[47] J.D.Swain[17] Z.Szillasi[42,¶] X.W.Tang[7] L.Tauscher[5] L.Taylor[11] C.Timmermans[30] Samuel C.C.Ting[14] S.M.Ting[14] S.C.Tonwar[10] J.Tóth[13] C.Tully[34] K.L.Tung[7]Y.Uchida[14] J.Ulbricht[47] E.Valente[35] G.Vesztergombi[13] I.Vetlitsky[27] D.Vicinanza[37] G.Viertel[47] S.Villa[11] M.Vivargent[4] S.Vlachos[5] I.Vodopianov[36] H.Vogel[33] H.Vogt[46] I.Vorobiev[16,27] A.A.Vorobyov[36] A.Vorvolakos[29] M.Wadhwa[5] W.Wallraff[1] M.Wang[14] X.L.Wang[19] Z.M.Wang[19] A.Weber[1] M.Weber[1] P.Wienemann[1] H.Wilkens[30] S.X.Wu[14] S.Wynhoff[1] L.Xia[31] Z.Z.Xu[19] B.Z.Yang[19] C.G.Yang[7] H.J.Yang[7] M.Yang[7] J.B.Ye[19] S.C.Yeh[50] J.M.You[33] An.Zalite[36] Yu.Zalite[36] P.Zemp[47] Z.P.Zhang[19] G.Y.Zhu[7] R.Y.Zhu[31] A.Zichichi[9,16,17] F.Ziegler[46] G.Zilizi[42,¶] M.Zöller[1]

1   I. Physikalisches Institut, RWTH, D-52056 Aachen, FRG[§]
    III. Physikalisches Institut, RWTH, D-52056 Aachen, FRG[§]
2   National Institute for High Energy Physics, NIKHEF, and University of Amsterdam, NL-1009 DB Amsterdam, The Netherlands
3   University of Michigan, Ann Arbor, MI 48109, USA
4   Laboratoire d'Annecy-le-Vieux de Physique des Particules, LAPP,IN2P3-CNRS, BP 110, F-74941 Annecy-le-Vieux CEDEX, France
5   Institute of Physics, University of Basel, CH-4056 Basel, Switzerland
6   Louisiana State University, Baton Rouge, LA 70803, USA
7   Institute of High Energy Physics, IHEP, 100039 Beijing, China[△]
8   Humboldt University, D-10099 Berlin, FRG[§]
9   University of Bologna and INFN-Sezione di Bologna, I-40126 Bologna, Italy
10 Tata Institute of Fundamental Research, Bombay 400 005, India
11 Northeastern University, Boston, MA 02115, USA
12 Institute of Atomic Physics and University of Bucharest, R-76900 Bucharest, Romania
13 Central Research Institute for Physics of the Hungarian Academy of Sciences, H-1525 Budapest 114, Hungary[‡]
14 Massachusetts Institute of Technology, Cambridge, MA 02139, USA
15 INFN Sezione di Firenze and University of Florence, I-50125 Florence, Italy
16 European Laboratory for Particle Physics, CERN, CH-1211 Geneva 23, Switzerland
17 World Laboratory, FBLJA Project, CH-1211 Geneva 23, Switzerland
18 University of Geneva, CH-1211 Geneva 4, Switzerland
19 Chinese University of Science and Technology, USTC, Hefei, Anhui 230 029, China[△]
20 SEFT, Research Institute for High Energy Physics, P.O. Box 9, SF-00014 Helsinki, Finland
21 University of Lausanne, CH-1015 Lausanne, Switzerland
22 INFN-Sezione di Lecce and Universitá Degli Studi di Lecce, I-73100 Lecce, Italy
23 Los Alamos National Laboratory, Los Alamos, NM 87544, USA
24 Institut de Physique Nucléaire de Lyon, IN2P3-CNRS,Université Claude Bernard, F-69622 Villeurbanne, France
25 Centro de Investigaciones Energéticas, Medioambientales y Tecnologícas, CIEMAT, E-28040 Madrid, Spain[♭]
26 INFN-Sezione di Milano, I-20133 Milan, Italy
27 Institute of Theoretical and Experimental Physics, ITEP, Moscow, Russia
28 INFN-Sezione di Napoli and University of Naples, I-80125 Naples, Italy
29 Department of Natural Sciences, University of Cyprus, Nicosia, Cyprus
30 University of Nijmegen and NIKHEF, NL-6525 ED Nijmegen, The Netherlands
31 California Institute of Technology, Pasadena, CA 91125, USA
32 INFN-Sezione di Perugia and Universitá Degli Studi di Perugia, I-06100 Perugia, Italy
33 Carnegie Mellon University, Pittsburgh, PA 15213, USA
34 Princeton University, Princeton, NJ 08544, USA
35 INFN-Sezione di Roma and University of Rome, "La Sapienza", I-00185 Rome, Italy
36 Nuclear Physics Institute, St. Petersburg, Russia
37 University and INFN, Salerno, I-84100 Salerno, Italy
38 University of California, San Diego, CA 92093, USA
39 Dept. de Fisica de Particulas Elementales, Univ. de Santiago, E-15706 Santiago de Compostela, Spain
40 Bulgarian Academy of Sciences, Central Lab. of Mechatronics and Instrumentation, BU-1113 Sofia, Bulgaria
41 Center for High Energy Physics, Adv. Inst. of Sciences and Technology, 305-701 Taejon, Republic of Korea
42 University of Alabama, Tuscaloosa, AL 35486, USA
43 Utrecht University and NIKHEF, NL-3584 CB Utrecht, The Netherlands
44 Purdue University, West Lafayette, IN 47907, USA
45 Paul Scherrer Institut, PSI, CH-5232 Villigen, Switzerland
46 DESY-Institut für Hochenergiephysik, D-15738 Zeuthen, FRG
47 Eidgenössische Technische Hochschule, ETH Zürich, CH-8093 Zürich, Switzerland
48 University of Hamburg, D-22761 Hamburg, FRG
49 National Central University, Chung-Li, Taiwan, China
50 Department of Physics, National Tsing Hua University, Taiwan, China
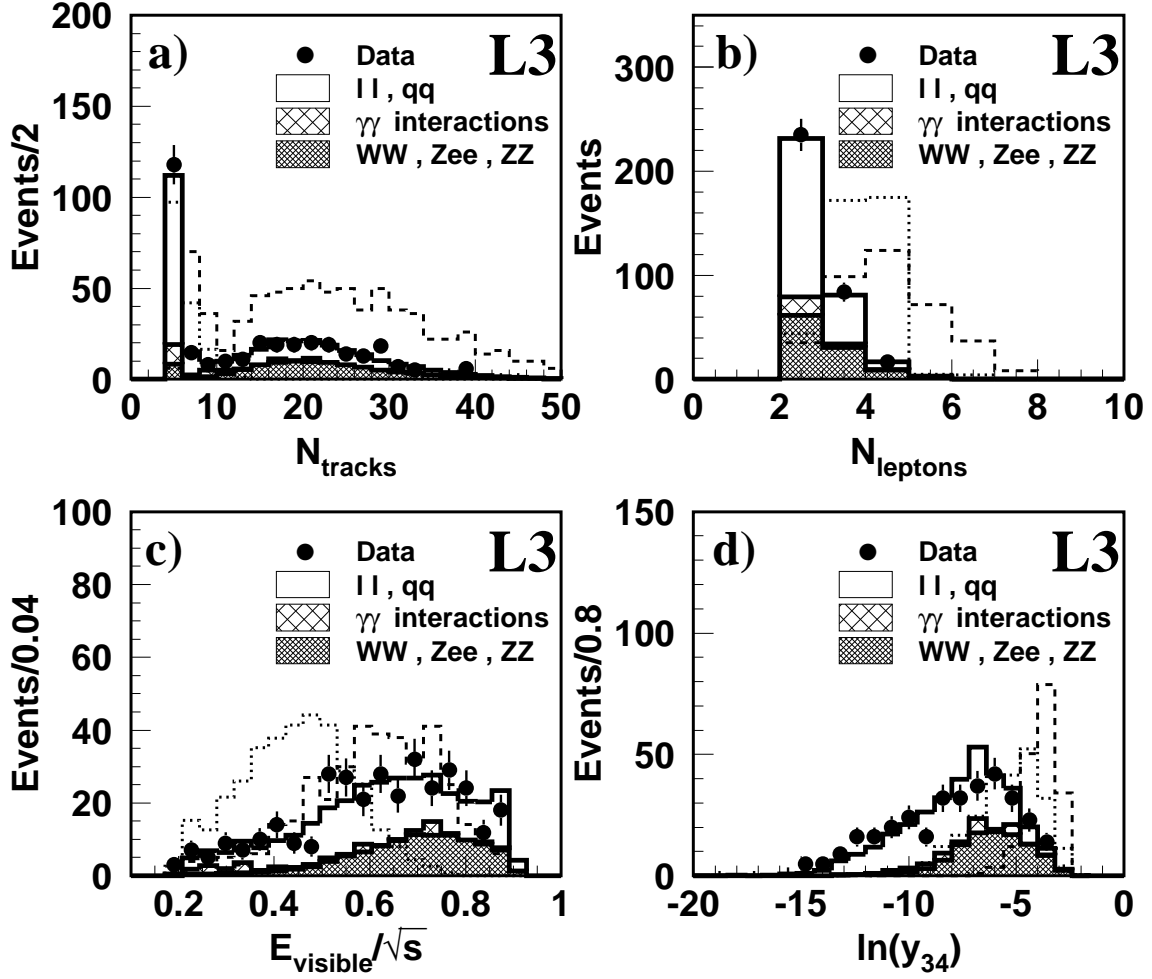
Figure 1: Distributions of a) the number of tracks, b) the number of leptons, c) the normalised visible energy and d) $\ln(y_{34})$ after the λ_{ijk} preselection. The solid histograms show the normalised sum of Standard Model processes. The dotted and dashed histograms show two examples of signal, with dominant coupling λ_{133}. The dotted histograms represent the process $e^+e^- \to \tilde{\chi}_1^0\tilde{\chi}_1^0$, for $M_{\tilde{\chi}_1^0} = 91$ GeV, corresponding to one hundred times the expected cross section. The dashed ones represent $e^+e^- \to \tilde{\chi}_1^+\tilde{\chi}_1^-$, with $M_{\tilde{\chi}_1^\pm} = 91$ GeV and $\Delta M = 50$ GeV, corresponding to four times the expected cross section.
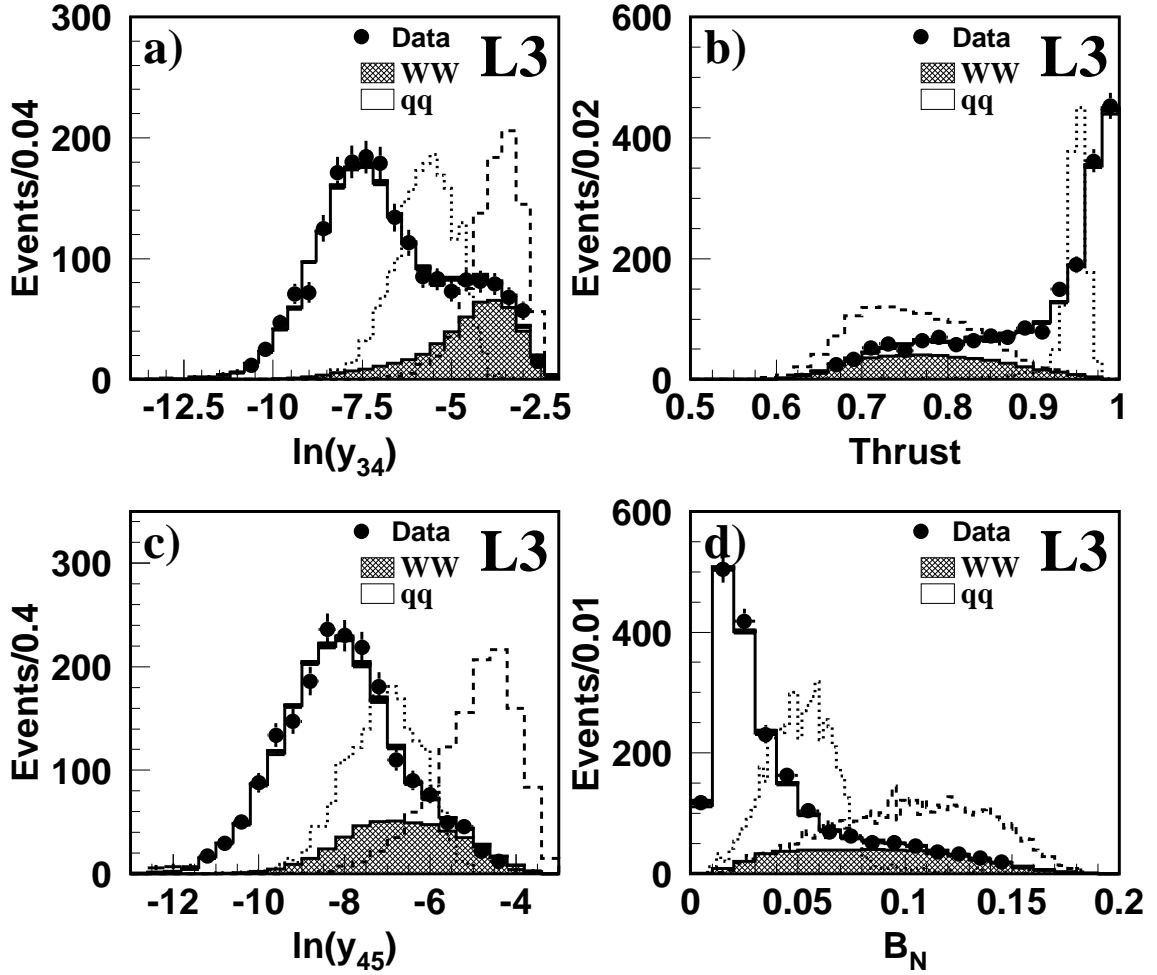
14

Figure 2: Distributions of a) $\ln(y_{34})$, b) thrust, c) $\ln(y_{45})$ and d) the narrow jet broadening after the λ''_{ijk} preselection. The solid histograms show Standard Model processes at $\sqrt{s} = 183$ GeV. The dashed and dotted histograms show two examples of signal, with dominant coupling λ''_{112}. The dashed histograms represent the process $e^+e^- \to \tilde{\chi}^0_1 \tilde{\chi}^0_1$, with $M_{\tilde{\chi}^0_1} = 90$ GeV, corresponding to five hundred times the expected cross section. The dotted ones represent the same process, with $M_{\tilde{\chi}^0_1} = 30$ GeV, corresponding to twenty times the expected cross section.
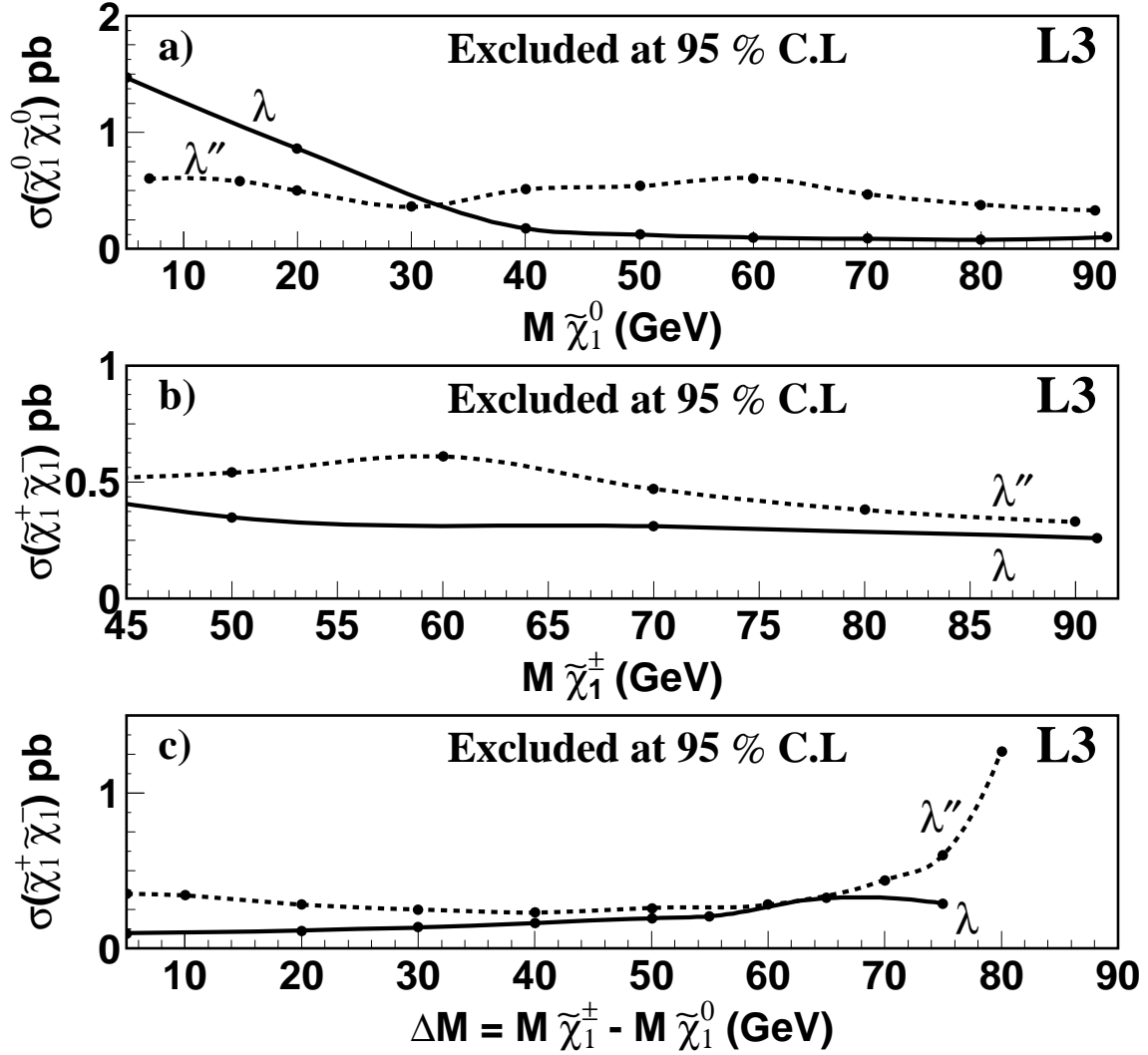
15

Figure 3: 95% C.L. upper limits on: a) the neutralino production cross section as a function of the neutralino mass, b) the chargino production cross section as a function of the chargino mass, in the direct decay mode and c) the chargino production cross section as a function of ΔM, for $M_{\widetilde{\chi}_1^\pm} = 91$ GeV, in the indirect decay mode. The solid lines show the limits obtained by the $\lambda_{ijk} = \lambda_{133}$ analysis, and the dashed lines show those obtained by the $\lambda''_{ijk} = \lambda''_{112}$ analysis.
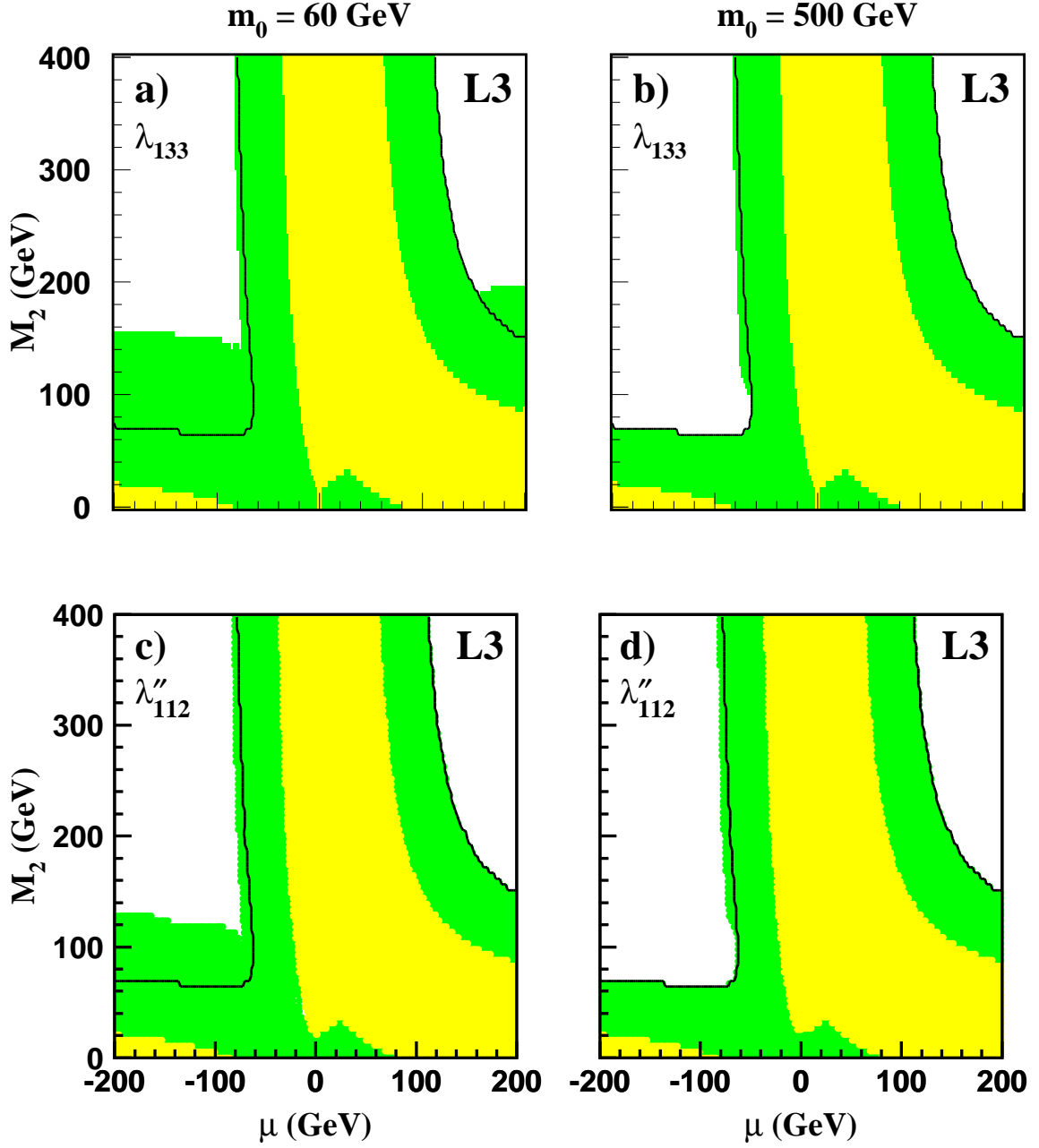
Figure 4: Exclusion regions at 95% confidence level for $\lambda_{ijk} = \lambda_{133}$ (a–b) and $\lambda''_{ijk} = \lambda''_{112}$ (c–d), for $\tan\beta = \sqrt{2}$ and $m_0 = 60$ GeV (a–c) or 500 GeV (b–d). The light grey region is excluded by the Z lineshape measurements and the dark grey region by the present analyses. The black solid lines indicate the chargino kinematic limit. The grey region beyond the kinematic limit is excluded by neutralino analyses.
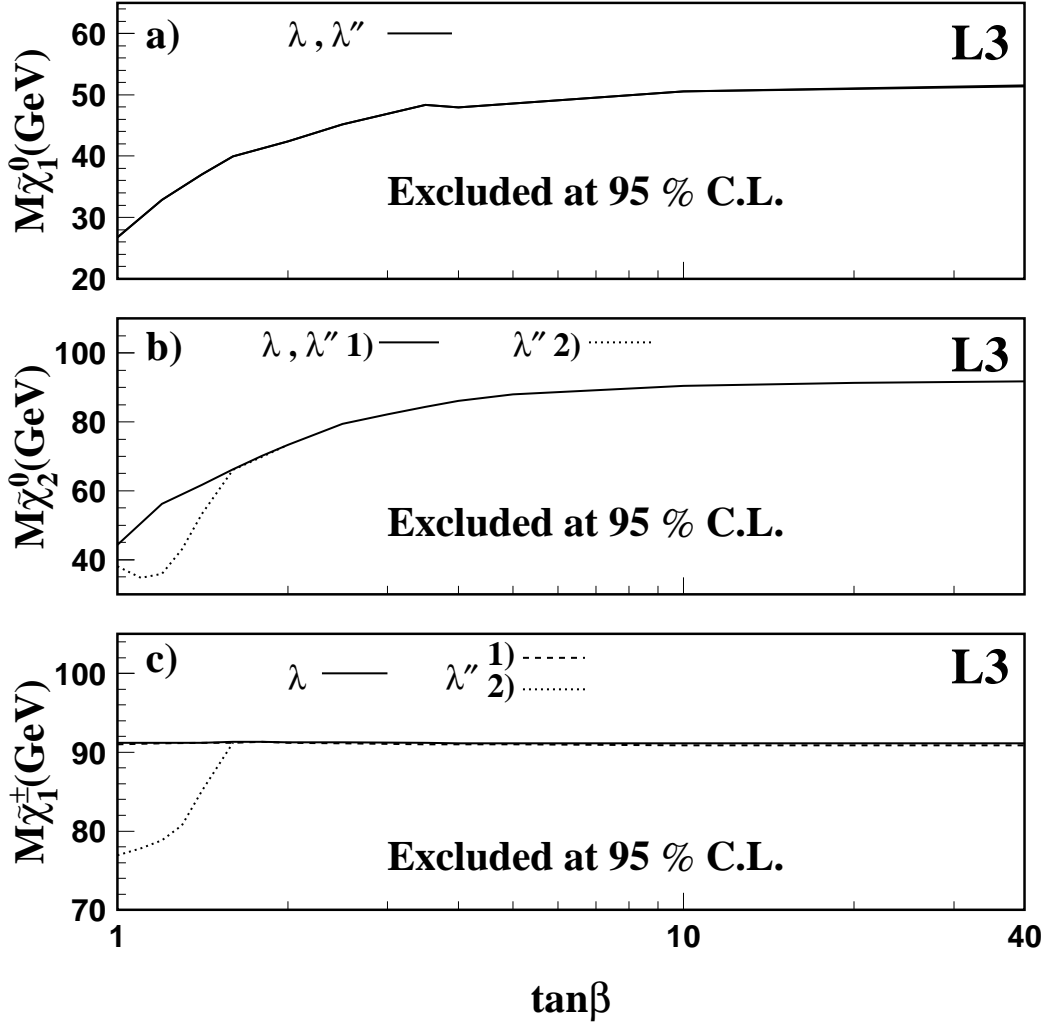
Figure 5: 95% C.L. lower limits on the masses of $\tilde{\chi}_1^0$ (a), $\tilde{\chi}_2^0$ (b) and $\tilde{\chi}_1^\pm$ (c), as a function of $\tan\beta$, for $0 \leq m_0 \leq 500$ GeV, $0 \leq M_2 \leq 2000$ GeV and -500 GeV $\leq \mu \leq 500$ GeV. The solid lines show the limit obtained by the λ_{133} analysis, the dashed lines by the λ''_{112} analysis in region 1) and the dotted lines by the λ''_{112} analysis in region 2).
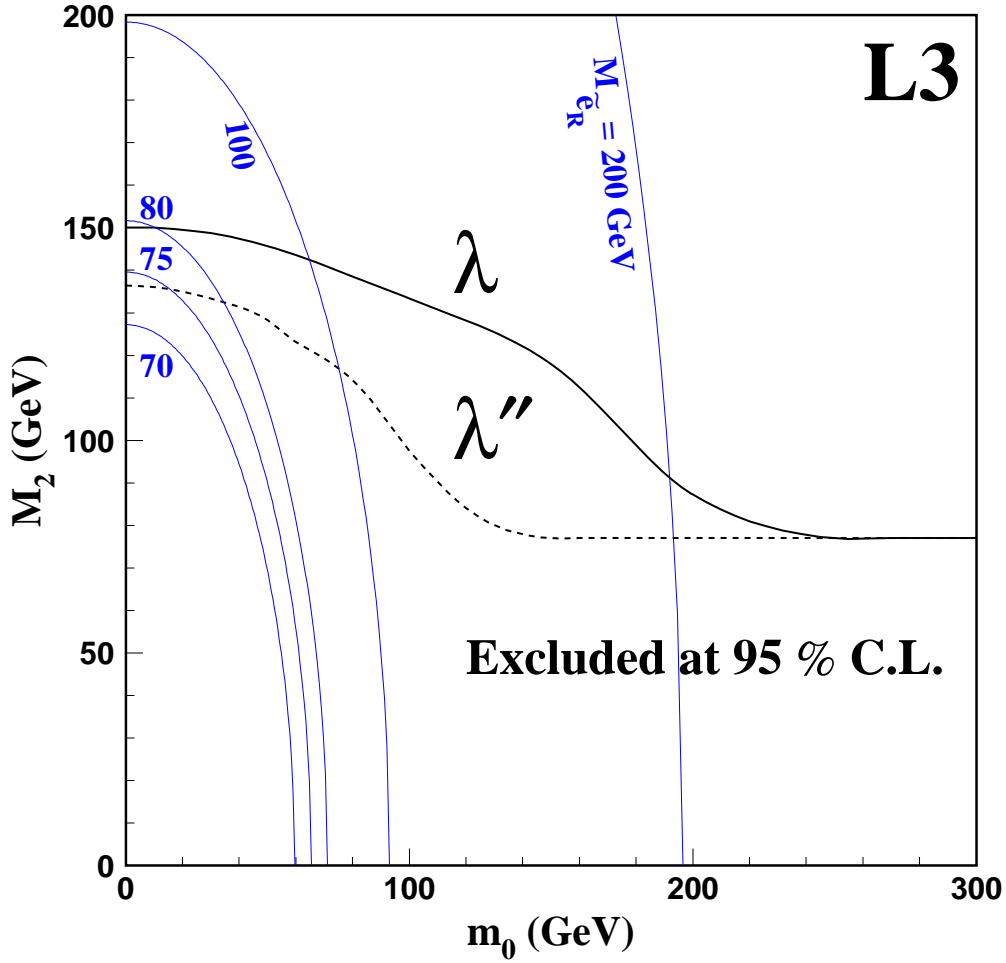
Figure 6: 95% C.L. exclusion contours in the $M_2 - m_0$ plane, for $\tan\beta = 2$. The lines labelled with the corresponding value in GeV represent the contours of constant scalar electron mass. The solid and dotted curves show the 95% C.L. lower limits on M_2 as a function of m_0, from which we derive the limits on the scalar electron mass.
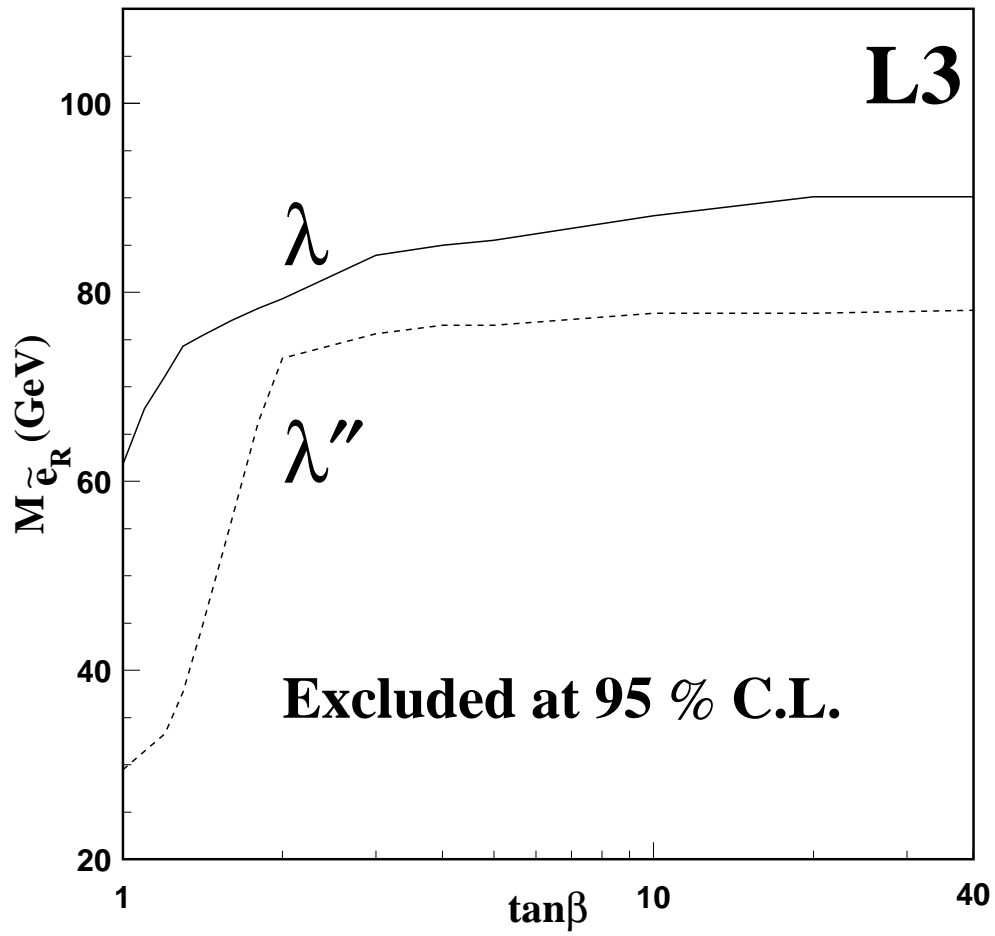
Figure 7: 95% C.L. lower limit on the mass of the scalar electron as a function of $\tan\beta$, for any value of μ, M_2 and m_0.